J Neurosurg Spine 13:267–275, 2010

Symptomatic relevance of intravertebral cleft in patients with osteoporotic vertebral fracture

Clinical article

Satoshi Kawaguchi, M.D.,[1] Keiko Horigome, M.D.,[1] Hideki Yajima, M.D.,[1] Takashi Oda, M.D.,[1] Yuichiro Kii, M.D.,[1] Kazunori Ida, M.D.,[2] Mitsunori Yoshimoto, M.D.,[2] Kousuke Iba, M.D.,[2] Tsuneo Takebayashi, M.D.,[2] and Toshihiko Yamashita, M.D.[2]

[1]Department of Orthopaedic Surgery, Asahikawa Kosei Hospital, Asahikawa; and [2]Department of Orthopaedic Surgery, Sapporo Medical University School of Medicine, Sapporo, Japan

Object. The present study was designed to determine clinical and radiographic characteristics of unhealed osteoporotic vertebral fractures (OVFs) and the role of fracture mobility and an intravertebral cleft in the regulation of pain symptoms in patients with an OVF.

Methods. Patients who had persistent low-back pain for 3 months or longer and a collapsed thoracic or lumbar vertebra that had an intervertebral cleft and abnormal mobility were referred to as having unhealed OVFs. Twenty-four patients with an unhealed OVF and 30 patients with an acute OVF were compared with regard to several clinical and radiographic features including the presence of an intravertebral fluid sign. Subsequently, the extent of dynamic mobility of the fractured vertebra was analyzed for correlation with the patients' age, duration of symptoms, back pain visual analog scale (VAS) score, and performance status. Finally, in cases of unhealed OVFs, the subgroup of patients with positive fluid signs was compared with the subgroup of patients with negative fluid signs.

Results. Patients with an unhealed OVF were more likely to have a crush-type fracture, shorter vertebral height of the fractured vertebra, and a fracture with a positive fluid sign than those with an acute OVF. The extent of dynamic mobility of the vertebra correlated significantly with the VAS score in patients with an unhealed OVF. In addition, a significant correlation with the extent of dynamic vertebral mobility with performance status was seen in patients with an unhealed OVF and those with an acute OVF. Of the 24 patients with an unhealed OVF, 14 had a positive fluid sign in the affected vertebra. Patients with a positive fluid sign exhibited a statistically significantly greater extent of dynamic vertebral mobility, a higher VAS score, a higher performance status grade, and a greater likelihood of having a crush-type fracture than those with a negative fluid sign. All but 1 patient with an unhealed OVF and a positive fluid sign had an Eastern Cooperative Oncology Group Performance Status Grade 3 or 4 (bedridden most or all of the time). In sharp contrast, all 10 patients with an unhealed OVF and a negative fluid sign were Grade 1 or 2.

Conclusions. Unhealed OVFs form a group of fractures that are distinct from acute OVFs regarding radiographic morphometry and contents of the intravertebral cleft. Dynamic vertebral mobility serves as a primal pain determinant in patients with an unhealed OVF and potentially in those with an acute OVF. Fluid accumulation in the intravertebral cleft of unhealed OVFs likely reflects long-term bedridden positioning of the patients in daily activity.
(DOI: 10.3171/2010.3.SPINE09364)

Key Words • **vertebral fracture** • **intravertebral cleft** • **mobility** • **osteoporosis** • **back pain**

Vertebral fractures are the most common type of osteoporotic fracture.[21] In the majority of patients with OVFs, acute back pain symptoms abate over a period of 6–8 weeks in line with the pace of fracture healing. However, a certain number of patients suffer persistent pain symptoms following an OVF. Various synonyms for this condition have been used in the literature, including Kümmell disease, avascular necrosis of the vertebra, vertebral fracture with intravertebral cleft, vertebral fracture with intraosseous vacuum phenomena, delayed vertebral collapse, vertebral pseudarthrosis, and intravertebral pseudarthrosis.[5,7,8,10,22] A common radiographic feature of the fractured vertebra in this group of patients is the presence of an intravertebral cleft that

Abbreviations used in this paper: ECOG = Eastern Cooperative Oncology Group; OVF = osteoporotic vertebral fracture; VAS = visual analog scale.

shows abnormal mobility. Although the primary pathogenesis of this condition is currently considered to be a failure of the fracture healing process, controversies exist regarding its nature, diagnosis, and therapeutic aspects.

Intravertebral clefts, also called intravertebral vacuum phenomena and Kümmell signs, have been well documented in the imaging literature.[1,3,16,18,24,26,28] In radiographs, they are seen as an intravertebral transverse, linear, or semilunar radiolucent shadow. Magnetic resonance images reveal an accumulation of air or fluid in the cleft.[10,14,28] Abnormal mobility of the intravertebral cleft has been suggested as a cause of severe back pain during motion in patients with vertebral pseudarthrosis.[8,18] However, to our knowledge no study has addressed the symptomatic relevance of the intravertebral cleft. Furthermore, the clinical significance of fluid and gas accumulation in the intravertebral cleft remains under debate.[10,14,28]

In the present study, we determined the diagnostic criteria of OVFs that failed to heal properly. We then compared patients with an unhealed OVF with those with an acute OVF with regard to clinical and radiographic features. Subsequently, we analyzed the symptomatic relevance of vertebral mobility and the intravertebral clefts in these groups of patients.

Methods

Patient Population

Patients with low-back pain lasting 3 months or longer, a collapsed vertebra in the thoracic or lumbar spine showing mobility in flexion-extension or sitting-supine position radiographs, and an air- or fluid-containing intravertebral cleft in the collapsed vertebra were considered to have an unhealed OVF. Between June 2005 and November 2008, 24 patients met the diagnostic criteria of an unhealed OVF and were treated at our institutions (Table 1). There were 17 women and 7 men with a mean age of 77.0 years (range 61–92 years). Two patients were younger than 65 years old. One of these patients (61 years old) had been treated with prednisolone for rheumatoid arthritis, and the other (62 years old) suffered a compression fracture caused by a fall from a height of 1.5 m 6 months before referral to our institution. The affected vertebrae were distributed from T-11 to L-4. The duration of back pain symptoms ranged from 3 to 48 months (mean 9.3 months).

As a control group, records of patients in whom an OVF had been diagnosed on plain radiographs and MR images obtained within 14 days after onset were reviewed. These fractures were referred to as acute OVFs. For the detection of an acute OVF, sagittal T1-weighted images, sagittal T2-weighted images, and sagittal STIR sequence images were used. Fractures caused by severe trauma and pathological fractures (tumor or infection) were excluded. Between May 2007 and April 2008, an acute OVF was diagnosed in 30 patients at one of our institutions. There were 21 women and 9 men with a mean age of 77.9 years (range 54–94 years) (Table 1). Two of 3 patients younger than 65 years old (ages 54 and 60 years) had been treated with corticosteroids for dermatomyositis and aplastic anemia, respectively. Fractures were distributed from the T-7 to L-4 vertebrae. Seventeen fractures were caused by a simple fall, and 13 fractures occurred during daily activities.

TABLE 1: Clinical pictures of patients with an unhealed OVF and those with an acute OVF*

Variable	Unhealed OVF	Acute OVF
no. of patients	24	30
age (yr)	77.0 ± 8.6	77.9 ± 9.4
male sex	7 (29)	9 (30)
location		
T1–10	0 (0)	5 (17)
T-11, T-12, & L-1	16 (67)	18 (60)
L2–5	8 (33)	7 (23)
duration of pain	9.3 ± 9.9 mos	4.1 ± 3.0 days
VAS score (mm)	61.0 ± 22.3	ND
ECOG Performance Status Grade		
1	10 (42)	0 (0)
2	1 (4)	9 (30)
3	8 (33)	19 (63)
4	5 (21)	2 (7)
fracture type		
normal	0 (0)	1 (3)
wedge	12 (50)	27 (90)
biconcave	1 (4)	2 (6)
crush	11 (46)	0 (0)
height of the vertebra (mm)		
sitting	8.1 ± 3.7†	17.1 ± 4.4†
supine	15.7 ± 4.6†	23.3 ± 4.5†
mobility	7.6 ± 3.6	5.2 ± 3.0
presence of prevalent fracture(s)	15 (63)	13 (43)
positive fluid sign	14 (59)†	3 (10)†

* Values for age, duration of pain, VAS score, and height of the vertebra are described as mean ± SD. All other values are the number of patients with percentages in parentheses. Abbreviation: ND = not determined.

† Statistically significant difference between unhealed OVFs and acute OVFs ($p < 0.01$).

Evaluation

Patients with an unhealed OVF were evaluated for severity of low-back pain by using the VAS and ECOG Performance Status.[20] In accordance with the ECOG Performance Status grade, Grade 1 indicates symptomatic but fully ambulatory, Grade 2 indicates symptomatic and up and about for more than 50% of waking hours, Grade

TABLE 2: Clinical relevance of the fluid sign in patients with an unhealed OVF*

Variable	Fluid Sign	
	Positive (14 patients)	Negative (10 patients)
patient age (yrs)	79.7 ± 9.3	73.1 ± 6.7
male sex	4 (29)	3 (30)
duration of pain (mos)	8.2 ± 6.7	10.9 ± 13.9
VAS score (mm)	74.9 ± 16.1†	41.4 ± 15.0†
ECOG Performance Status Grade	3.2 ± 0.8†	1.1 ± 0.3†
crush-type fracture	10 (71)†	1 (10)†
height on sitting radiographs (mm)	8.3 ± 3.9	7.8 ± 3.9
height on supine radiographs (mm)	17.5 ± 4.7	13.6 ± 3.9
dynamic mobility (mm)	9.2 ± 4.1‡	5.8 ± 1.9‡
presence of prevalent fracture	9 (64)	6 (60)
communication to intradiscal air	2 (17)†	10 (100)†

* Values for age, duration of pain, VAS score, performance status, and height of anterior wall are described as the mean ± SD. All other values are the number of patients with percentages in parentheses.
† Statistically significant difference ($p < 0.01$) between the subgroups with positive and negative fluid signs.
‡ Statistically significant difference ($p < 0.05$) between the subgroups with positive and negative fluid signs.

3 indicates symptomatic and being confined to bed or a chair for 50% or more of waking hours, and Grade 4 indicates being totally confined to bed or a chair. Patients with an acute OVF were also evaluated for performance status.

Radiographic evaluation included classification of the fracture types, dynamic mobility of the affected vertebra, contents of the intravertebral cleft, prevalent vertebral fracture, and communication between air in the intravertebral cleft and air in the adjacent intervertebral disc. Fractures were classified into normal, wedge, biconcave, and crush types[4,6] using lateral decubitus-position radiographs (Fig. 1A).

Dynamic mobility of the vertebra was determined by measuring the height of the affected vertebra manually in lateral radiographs obtained in the sitting and supine positions (Fig. 1B and C).[17] The radiographs were obtained at a film-focus distance of 1.1 m during the initial visit. Sitting lateral radiographs (Fig. 1B) and supine cross-table lateral radiographs (Fig. 1C) were compared with regard to the vertebral height that was measured to the nearest millimeter at the anterior border, the midpoint, and the posterior border of the vertebra. The region that indicated the largest difference of the vertebral height between the sitting lateral radiograph and the supine cross-table lateral radiograph was selected. The difference in the vertebral height in that region was referred to as the dynamic mobility of the vertebra. All cases with an acute OVF and 22 of 24 cases with an unhealed fracture were evaluated for dynamic fracture mobility using the aforementioned procedure.

Accumulation of fluid in fractured vertebrae (fluid sign) was determined using MR imaging. In cases in which the signal intensity of an intravertebral lesion was equivalent to that of CSF on T2-weighted images, the vertebrae were defined as having a positive fluid sign. Intravertebral air and intradiscal air were defined as profound low-density lesions on sagittal reconstructed CT scans. Presence of intravertebral air, intradiscal air (vacuum disc), and communication between these 2 air lesions were determined using serial sagittal images of CT scans. A fluid sign was assessed in all 54 patients.

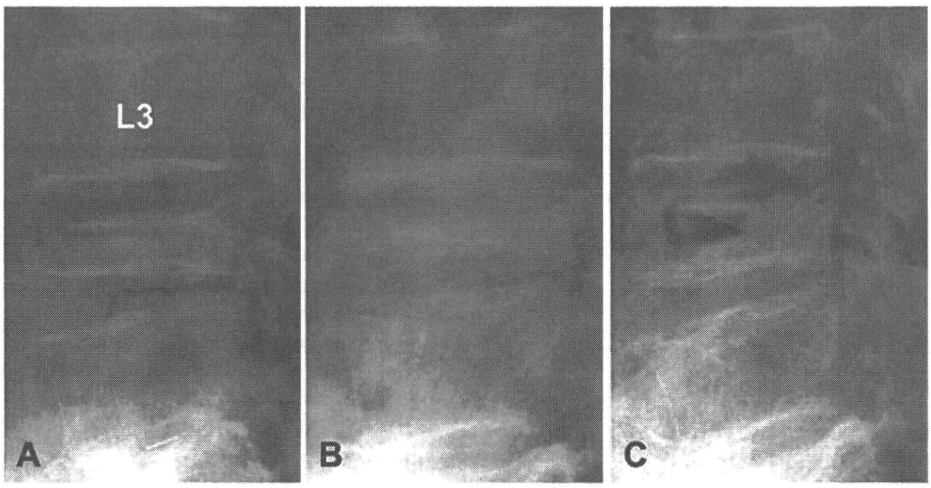

Fig. 1. Evaluation of fracture type and dynamic mobility. This 91-year-old man had an unhealed fracture of the L-4 vertebra. Fractures are classified into normal, wedge, biconcave, and crush types by using lateral decubitus-position radiographs **(A)**. The present case is classified as a crush type. The difference in the vertebral height at the anterior border of the affected vertebra between a sitting lateral radiograph **(B)** and a supine cross-table lateral radiograph **(C)** indicates the extent of dynamic fracture mobility. In the present case, the vertebral height is 7 mm in the sitting lateral radiograph and 21 mm in the supine lateral radiograph, indicating a dynamic fracture mobility of 14 mm.

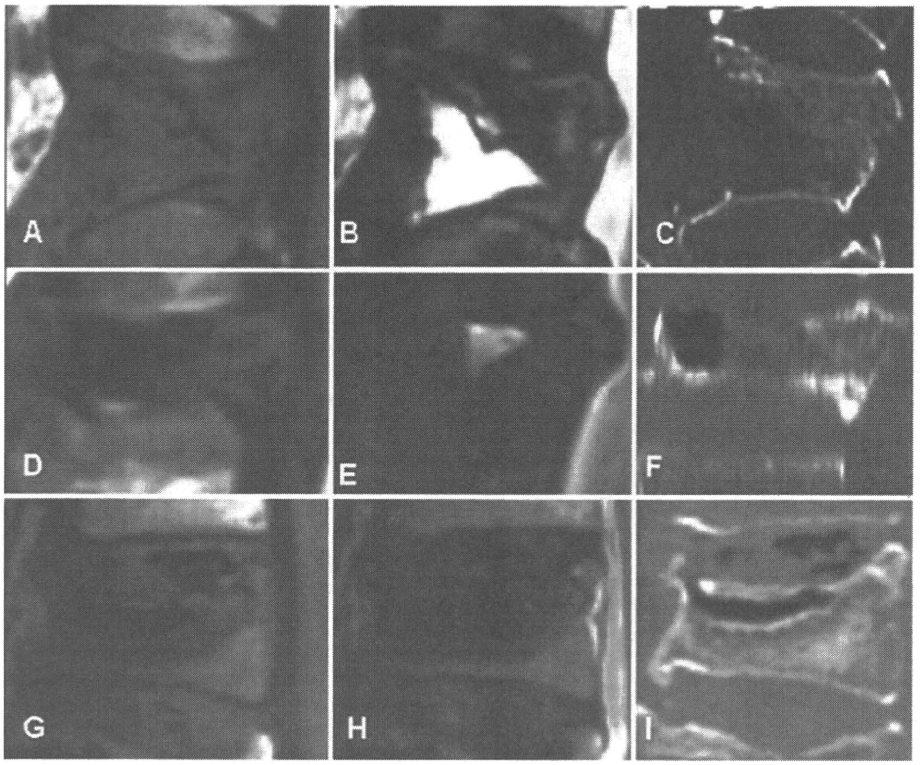

Fig. 2. Representative T1-weighted MR images **(A, D, and G)**, T2-weighted MR images **(B, E, and H)**, and reconstructed CT scans **(C, F, and I)** of unhealed OVFs. **A–C:** Images obtained in an 89-year-old man with an unhealed crush-type fracture of the T-12 vertebra, showing an accumulation of fluid in the intravertebral cleft. There is a fracture line in the posterior wall of the T-12 vertebra, associated with a collapse of both anterior and posterior borders of the vertebra. Of our cases, 9 exhibited an accumulation of fluid alone in the cleft. **D–F:** Images obtained in a 68-year-old man with an unhealed crush-type fracture of the L-1 vertebra, showing an accumulation of fluid and air in the intravertebral cleft. There is a fracture line in the posterior wall of the L-1 vertebra, associated with a collapse of both anterior and posterior borders of the vertebra. Of our cases, 5 had fluid and air in the cleft. **G–I:** Images obtained in a 67-year-old man with an unhealed wedge-type fracture of the T-12 vertebra, showing a negative fluid sign. The intravertebral cleft is filled with air. The posterior wall of the vertebra has not collapsed, consistent with a wedge-type fracture. Of our cases, 10 showed an accumulation of air alone in the cleft (negative fluid sign).

Intravertebral air was evaluated using CT scans in 22 of 24 patients with an unhealed OVF. Prevalent vertebral fractures were defined by MR images showing collapse with recovered signal intensity (high signal intensity on T1- and T2-weighted images). All MR and CT images were analyzed by an author (S.K.) and an experienced radiologist working together.

Analysis of Patient Groups

Patients with an unhealed OVF and those with an acute OVF were compared with regard to clinical and radiographic features, including age, sex, duration of pain, performance status, fracture location, fracture classification, height of the affected vertebra, extent of dynamic vertebral mobility, presence of a fluid sign, and presence of prevalent vertebral fractures.

The extent of dynamic mobility of the affected vertebra was analyzed for correlation with age, duration of symptoms, and performance status in all patients, and with VAS scores in patients with an unhealed OVF.

The OVFs were divided into 2 subgroups on the basis of a fluid sign. Two subgroups (positive fluid sign and negative fluid sign) were compared with regard to age, sex, duration of pain, VAS score, performance status, number of cases with a crush-type fracture, height of the affected vertebra, extent of dynamic fracture mobility, presence of prevalent vertebral fracture, and communication between intravertebral air and intradiscal air.

Statistical significance was determined using the Pearson correlation method, the Mann-Whitney test, and the Fisher exact probability test. A p value < 0.05 was considered statistically significant. Groups containing fewer than 5 patients were not subjected to statistical analysis.

Results

Clinical and Radiographic Features of Unhealed OVFs and Acute OVFs

To determine the clinical and radiographic features of unhealed OVFs, we analyzed 24 patients with putative diagnosis of an unhealed OVF and 30 patients with an

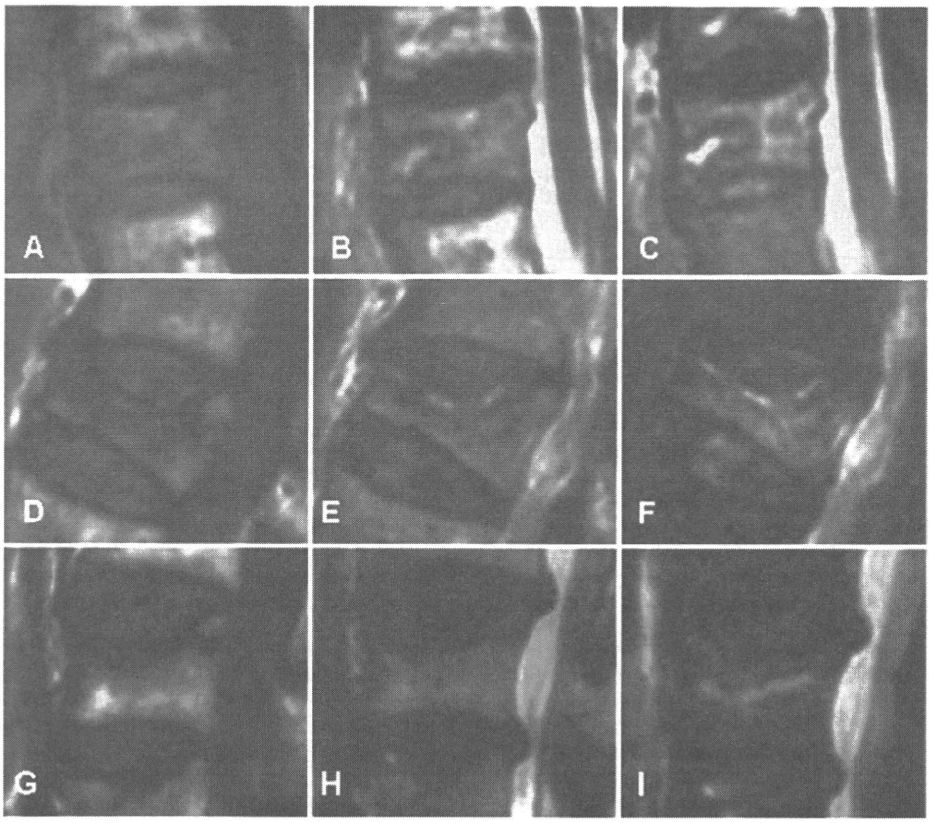

Fig. 3. Representative T1-weighted **(A, D, and G)**, T2-weighted **(B, E, and H)**, and STIR **(C, F, and I)** MR images of acute OVFs. The intravertebral high signal intensity in STIR images *(right panels)* indicates an edematous change associated with acute fracture. **A–C:** Images obtained in an 85-year-old woman with an acute wedge-type fracture of the T-11 vertebra, showing a square-shaped fluid sign. The posterior wall of the vertebra has not collapsed. Of our cases, only 1 showed a square-shaped fluid sign. **D–F:** Images obtained in an 80-year-old woman with an acute wedge-type fracture of the L-1 vertebra, showing a linear fluid sign. The posterior wall of the vertebra has not collapsed. Of our cases, 2 exhibited a linear fluid sign. **G–I:** Images obtained in an 84-year-old woman with an acute wedge-type fracture of the L-3 vertebra. There is no fluid sign in the vertebra. The posterior wall of the vertebra has not collapsed. Of our cases, 27 had a negative fluid sign.

acute OVF comparatively. As depicted in Table 1, age, sex, and location of the fractures were comparable between the groups. The VAS score of patients with an unhealed OVF ranged from 20 to 100 mm (mean 61 mm). The ECOG Performance Status was Grade 1 in 10 patients, Grade 2 in 1 patient, Grade 3 in 8 patients, and Grade 4 in 5 patients. In patients with an acute OVF, the performance status was Grade 2 in 9 patients, Grade 3 in 19 patients, and Grade 4 in 2 patients.

With respect to the fracture types, 12 patients with an unhealed OVF (50%) had a wedge-type fracture and 11 patients (46%) had a crush-type fracture (Figs. 1 and 2). In contrast, 27 patients with an acute OVF (90%) had a wedge-type fracture, and none of them had a crush-type fracture (Fig. 3). In sitting and supine cross-table lateral radiographs, the height of the affected vertebra was significantly shorter in unhealed OVFs than that in acute OVFs. The average mobility of the vertebra was 7.6 mm in unhealed OVFs and 5.2 mm in acute OVFs. The difference was not statistically significant. Prevalent fractures were found in 15 patients with an unhealed OVF (63%) and 13 patients with an acute OVF (43%).

Intravertebral Accumulation of Fluid and Air

Fourteen patients with an unhealed OVF (59%) and 3 patients with an acute OVF (10%) had a positive fluid sign in the affected vertebra (Table 1 and Figs. 2 and 3). The difference in the frequency of a positive fluid sign is statistically significant. Fluid was accumulated in a triangular/square shape in all 14 cases of an unhealed OVF (Fig. 2). In contrast, 2 of 3 acute OVFs showed fluid accumulation in a linear shape and the remaining fracture exhibited a triangular/square shape (Fig. 3). Accumulation of air in the vertebra was defined using reconstructed CT scans in 22 of 24 patients with an unhealed OVF. Of these, 5 patients showed fluid and air in the intravertebral cleft, and 10 patients had an air-filled intravertebral cleft (Fig. 2).

Correlation of Dynamic Vertebral Mobility With Clinical Parameters

Based on these clinical and radiographic findings, we conducted a correlation analysis between the extent of dynamic vertebral mobility and clinical parameters. In patients with an unhealed OVF, there was a significant

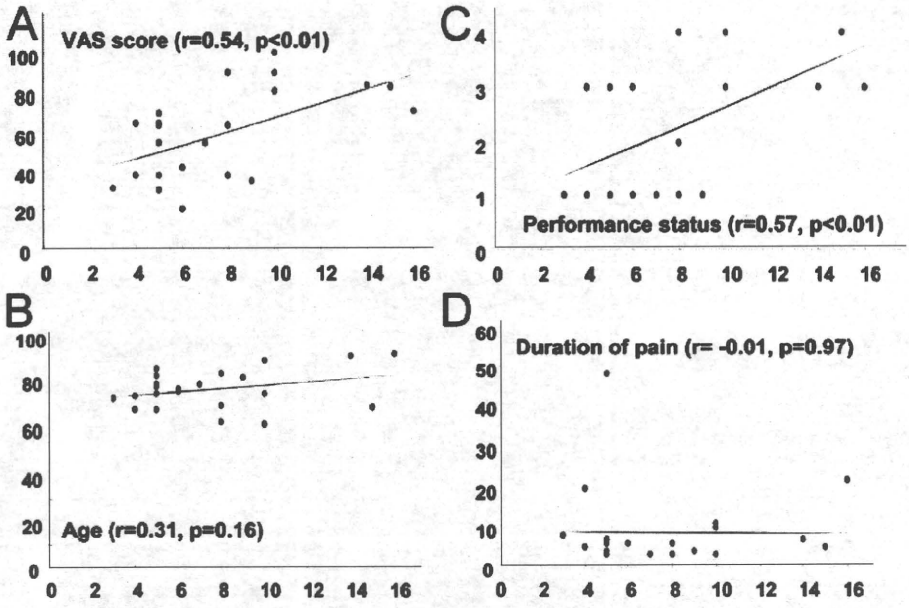

FIG. 4. Graphs showing the correlations of dynamic fracture mobility and clinical parameters in patients with an unhealed OVF. The x axes indicate dynamic mobility of the affected vertebra (mm). The y axes indicate VAS score (mm, **A**), ECOG Performance Status (grades, **B**), age (years, **C**), and duration of pain symptoms (months, **D**). The correlations of dynamic mobility with clinical parameters were analyzed and are presented with correlation coefficient (r) and probability (p) values.

correlation between the extent of dynamic mobility and the VAS score ($r = 0.54$, $p < 0.01$) (Fig. 4). A significant correlation was also seen between the extent of dynamic mobility and performance status ($r = 0.57$, $p < 0.01$) (Fig. 4). In contrast, the extent of dynamic mobility was not significantly correlated with the patient's age and duration of symptoms. In patients with an acute OVF (Fig. 5), statistically significant correlations were seen between the extent of dynamic fracture mobility and performance status ($r = 0.61$, $p < 0.01$) and the patient's age ($r = 0.49$, $p < 0.01$). Also, there was a reverse correlation between the extent of dynamic mobility and duration of symptoms ($r = -0.45$, $p < 0.02$) (Fig. 5).

Clinical Relevance of Intravertebral Fluid Sign

Finally, we analyzed the clinical relevance of the fluid sign. Because only 3 patients with an acute OVF showed a positive fluid sign, analysis focused on patients with an unhealed OVF. As depicted in Table 2, there was no statistically significant difference between the subgroup with a positive fluid sign and that with a negative fluid sign with respect to patients' age, sex, duration of symptoms, height of the affected vertebra in sitting and supine lateral radiographs, and the presence of prevalent fractures. In contrast, statistically significant differences were noted between these subgroups with respect to back pain VAS score, ECOG Performance Status grade, frequency of a crush-type fracture, extent of dynamic vertebral mobility, and frequency of communication between intravertebral air and intradiscal air. The VAS score, ECOG Performance Status grade, and the extent of dynamic vertebral mobility were larger in the subgroup with a positive fluid sign than that with a negative one. Notably, 13 of 14 patients with a positive fluid sign and an unhealed OVF had an ECOG Performance Status Grade 3 or 4, whereas all 10 patients with a negative fluid sign and an unhealed OVF had an ECOG Performance Status Grade 1 or 2. Communication between intradiscal air and intravertebral air was seen in all 10 patients with a negative fluid sign in an unhealed OVF and 2 of 12 patients with a positive fluid sign in an unhealed OVF examined with CT scans (Fig. 6).

Discussion

In the present study, we analyzed 24 patients with an unhealed OVF and 30 patients with an acute OVF. Patients with an unhealed OVF suffered various degrees of persistent pain for 3 months or longer and had a collapsed thoracic or lumbar vertebra that had an intravertebral cleft and mobility. Apart from these features, these patients were more likely to have a crush-type fracture, shorter vertebral height of the fractured vertebra, and a positive fluid sign fracture than those with an acute OVF. These findings support the claim that the fractures deemed as unhealed OVFs in this study form a distinct group of fractures from acute OVFs.

The extent of dynamic vertebral mobility correlated significantly with back pain status (VAS score) in patients with an unhealed OVF. Dynamic mobility of the vertebra has been speculated as a cause of pain symptoms in patients with an unhealed OVF.[8,18] This assumption is based on the observation that operative stabilization of the intravertebral mobility in patients with an unhealed OVF leads to immediate pain relief.[7,9,10] Our findings serve as a more direct support for this assumption. In addition,

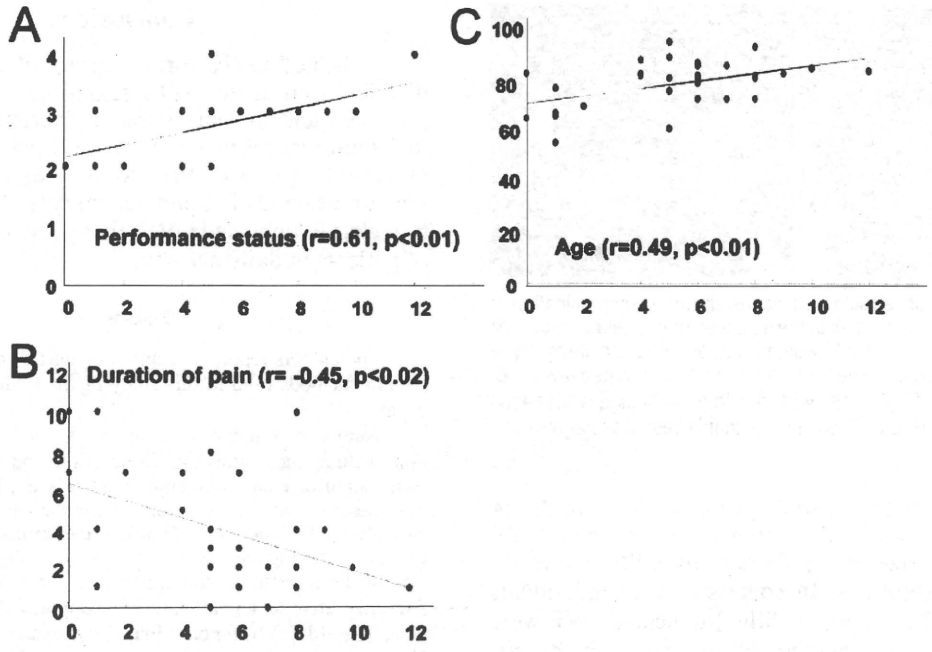

Fig. 5. Graph showing the correlations of dynamic fracture mobility and clinical parameters in patients with an acute OVF. The x axes indicate dynamic mobility of the affected vertebra (mm). The y axes indicate ECOG Performance Status (grades, **A**), age (years, **B**), and duration of pain symptoms (days, **C**). The correlations of dynamic mobility with clinical parameters were analyzed and are presented with correlation coefficient (r) and probability (p) values.

a significant correlation between the extent of dynamic fracture mobility and performance status grade was seen in patients with an unhealed OVF and those with an acute OVF. This indicates the possibility that dynamic fracture mobility serves as a primal pain determinant for patients with an unhealed OVF as well as those with an acute OVF.

The clinical significance of fluid accumulation in the intravertebral clefts remains under debate. In the literature, Yu et al.[28] reported that vertebral collapse was more advanced in cases of unhealed OVFs with a negative fluid sign (that is, those that are air-filled) than unhealed OVFs with a positive fluid sign. This indicates that the contents (air or fluid) of the intravertebral cleft represent the severity of the vertebral collapse on radiographs. In contrast, Jang et al.[10] suggested that the contents of the intravertebral cleft denote the "stages" of unhealed OVFs, where fluid is accumulated in the early stages and converted into air in the later stages. Malghem,[16] Sarli,[26] and Linn[15] and their colleagues reported that supine positioning for a long time (more than 20 minutes) leads to fluid collection in the intravertebral cleft. They speculated that fluid may flow from blood into the intravertebral cleft by negative pressure created by widening of the affected vertebra during supine positioning. In this respect, all but 1 patient with an unhealed OVF that had a positive fluid sign in the present study had an ECOG Performance Status Grade 3 or 4, indicating that these patients were bedridden most of the time. In sharp contrast, all 10 patients with an unhealed OVF that had a negative fluid sign had an ECOG Performance Status Grade 1 or 2. Therefore, fluid accumulation in unhealed OVFs likely reflects long-term bedridden positioning of the patients. This theory, however, does not explain our finding that 18 of 27 patients with an acute OVF with a negative fluid sign had an ECOG Performance Status Grade 3 or 4.

Communication between the intravertebral air and intradiscal air in the adjacent disc seen in the present study was previously reported by Lafforgue et al.[13] They found such communication in 83% of the 23 patients with an unhealed OVF with a negative fluid sign (air-filled). Lack of communication between the intravertebral cleft and intradiscal air in the adjacent disc in patients with an unhealed OVF was also demonstrated by Yu et al.[28] These observations, together with the findings in the present study, consistently suggest that the communication between the intravertebral cleft and the adjacent intradiscal air is likely to be pathognomic for air accumulation in the cleft.

Of 24 patients with an unhealed OVF, 14 patients (58%) had positive fluid signs (including 5 patients showing both fluid and air) and the remaining 10 patients (42%) exhibited an air-filled cleft in the present study group. Similarly, Yu et al.[28] reported a positive fluid sign in 61% (fluid alone in 40% and fluid and air in 21%) and a negative fluid sign (air-filled clefts) in the remaining 39% of 112 patients with an unhealed OVF. In contrast, in the studies by Jang et al.[10] and Lane et al.,[14] only 12.5% and 11.4%, respectively, of unhealed OVFs had an air-filled cleft. These low percentages of the air-filled types may be explained by the selection of patients as every participant in these studies was referred to them for percutane-

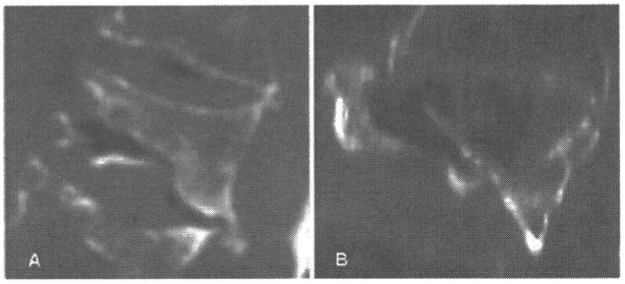

Fig. 6. Sagittal reconstructed CT scans showing communication of the air in the vertebra and the air in the adjacent intervertebral disc. **A:** Image obtained in a 67-year-old woman with an unhealed wedge-type fracture of the L-1 vertebra. The fluid sign in this case was negative. **B:** Image obtained in a 77-year-old woman with an unhealed wedge-type fracture of the L-3 vertebra. The fluid sign in this case was negative.

ous vertebroplasty. In our study group, all but 1 of the 14 patients with a positive fluid sign in an unhealed OVF had been hospitalized for pain and disability before referral to our institutions. In contrast, all 10 individuals with a negative fluid sign (air-filled) unhealed OVF were outpatients. Thus, the number of patients with the air-filled unhealed OVF is likely to be low in referral-based orthopedic clinics. Because patients with an air-filled unhealed OVF visit clinics with relatively mild back pain, it is important that they are not misdiagnosed. In fact, some of the patients in our study group had been treated for osteoporosis-related chronic back pain elsewhere before presenting to our institutions.

The presence of prevalent fractures may affect back pain status and performance status of patients with an acute OVF or an unhealed OVF. In this regard, frequency of the presence of prevalent fracture(s) was not significantly different between the patients with an unhealed OVF and those with an acute OVF (Table 1). Also, there was no significant difference in terms of frequency of prevalent fractures between unhealed OVFs with positive and negative fluid signs (Table 2). Patients who present for medical attention with back pain and have only a healed vertebral fracture may represent a suitable control group in the present study. However, in these patients, there is difficulty in determining whether healed OVF(s) are responsible for the pain symptoms.

Unhealed OVFs with small dynamic vertebral mobility may be treated successfully with the long-term wearing of a body jacket. However, in the literature, unhealed OVFs have been treated surgically rather than conservatively. A variety of surgical procedures have been reported for the treatment of unhealed OVFs. These include osteosynthesis,[9] decompression and fusion surgeries via anterior,[11,19] posterior,[12,19,25] and anteroposterior[27] approaches, percutaneous vertebroplasty,[2,10,23] and percutaneous kyphoplasty.[7] The treatment procedure was determined depending on the severity of the fracture and neurological compromise and the surgeon's preference. Whereas osteosynthesis and fusion surgeries aim at solid bone union for stabilization of the affected vertebra, union status following percutaneous vertebroplasty or percutaneous kyphoplasty has not yet been addressed.

Conclusions

Unhealed OVFs form a group of fractures that are distinct from acute OVFs regarding radiographic morphometry and contents of the intravertebral cleft. Dynamic fracture mobility serves as a primal pain determinant of patients with an unhealed OVF and potentially those with an acute OVF. Fluid accumulation in the intravertebral cleft in unhealed OVFs likely reflects the positioning of patients in daily activity.

Disclosure

The authors report no conflict of interest concerning the materials or methods used in this study or the findings specified in this paper.

Author contributions to the study and manuscript preparation include the following. Conception and design: Kawaguchi. Acquisition of data: Horigome, Yajima, Oda, Kii, Ida, Yoshimoto, Iba, Takebayashi. Analysis and interpretation of data: Kawaguchi, Horigome, Yajima, Oda. Drafting the article: Kawaguchi, Oda. Critically revising the article: Oda, Takebayashi. Reviewed final version of the manuscript and approved it for submission: all authors. Administrative/technical/material support: Horigome, Yajima, Oda, Kii, Ida, Yoshimoto, Iba, Takebayashi. Study supervision: Yamashita.

Acknowledgment

The authors thank Dr. M. Tamakawa for his support and comments on imaging analysis.

References

1. Bhalla S, Reinus WR: The linear intravertebral vacuum: a sign of benign vertebral collapse. **AJR Am J Roentgenol 170:** 1563–1569, 1998
2. Carlier RY, Gordji H, Mompoint DM, Vernhet N, Feydy A, Vallée C: Osteoporotic vertebral collapse: percutaneous vertebroplasty and local kyphosis correction. **Radiology 233:** 891–898, 2004
3. Dupuy DE, Palmer WE, Rosenthal DI: Vertebral fluid collection associated with vertebral collapse. **AJR Am J Roentgenol 167:**1535–1538, 1996
4. Eastell R, Cedel SL, Wahner HW, Riggs BL, Melton LJ III: Classification of vertebral fractures. **J Bone Miner Res 6:** 207–215, 1991
5. Freedman BA, Heller JG: Kummel disease: a not-so-rare complication of osteoporotic vertebral compression fractures. **J Am Board Fam Med 22:**75–78, 2009
6. Genant HK, Wu CY, van Kuijk C, Nevitt MC: Vertebral fracture assessment using a semiquantitative technique. **J Bone Miner Res 8:**1137–1148, 1993
7. Grohs JG, Matzner M, Trieb K, Krepler P: Treatment of intravertebral pseudarthroses by balloon kyphoplasty. **J Spinal Disord Tech 19:**560–565, 2006
8. Hasegawa K, Homma T, Uchiyama S, Takahashi H: Vertebral pseudarthrosis in the osteoporotic spine. **Spine 23:**2201–2206, 1998
9. Hasegawa K, Homma T, Uchiyama S, Takahashi HE: Osteosynthesis without instrumentation for vertebral pseudarthrosis in the osteoporotic spine. **J Bone Joint Surg Br 79:**452–456, 1997
10. Jang JS, Kim DY, Lee SH: Efficacy of percutaneous vertebroplasty in the treatment of intravertebral pseudarthrosis associated with noninfected avascular necrosis of the vertebral body. **Spine 28:**1588–1592, 2003
11. Kaneda K, Asano S, Hashimoto T, Satoh S, Fujiya M: The

treatment of osteoporotic-posttraumatic vertebral collapse using the Kaneda device and a bioactive ceramic vertebral prosthesis. **Spine 17 (8 Suppl):**S295–S303, 1992
12. Kim KT, Suk KS, Kim JM, Lee SH: Delayed vertebral collapse with neurological deficits secondary to osteoporosis. **Int Orthop 27:**65–69, 2003
13. Lafforgue P, Chagnaud C, Daumen-Legré V, Daver L, Kasbarian M, Acquaviva PC: The intravertebral vacuum phenomenon ("vertebral osteonecrosis"). Migration of intradiscal gas in a fractured vertebral body? **Spine 22:**1885–1891, 1997
14. Lane JI, Maus TP, Wald JT, Thielen KR, Bobra S, Luetmer PH: Intravertebral clefts opacified during vertebroplasty: pathogenesis, technical implications, and prognostic significance. **AJNR Am J Neuroradiol 23:**1642–1646, 2002
15. Linn J, Birkenmaier C, Hoffmann RT, Reiser M, Baur-Melnyk A: The intravertebral cleft in acute osteoporotic fractures: fluid in magnetic resonance imaging-vacuum in computed tomography? **Spine 34:**E88–E93, 2009
16. Malghem J, Maldague B, Labaisse MA, Dooms G, Duprez T, Devogelaer JP, et al: Intravertebral vacuum cleft: changes in content after supine positioning. **Radiology 187:**483–487, 1993
17. McKiernan F, Faciszewski T: Intravertebral clefts in osteoporotic vertebral compression fractures. **Arthritis Rheum 48:** 1414–1419, 2003
18. Mirovsky Y, Anekstein Y, Shalmon E, Peer A: Vacuum clefts of the vertebral bodies. **AJNR Am J Neuroradiol 26:**1634–1640, 2005
19. Mochida J, Toh E, Chiba M, Nishimura K: Treatment of osteoporotic late collapse of a vertebral body of thoracic and lumbar spine. **J Spinal Disord 14:**393–398, 2001
20. Oken MM, Creech RH, Tormey DC, Horton J, Davis TE, McFadden ET, et al: Toxicity and response criteria of the Eastern Cooperative Oncology Group. **Am J Clin Oncol 5:**649–655, 1982
21. Papaioannou A, Watts NB, Kendler DL, Yuen CK, Adachi JD, Ferko N: Diagnosis and management of vertebral fractures in elderly adults. **Am J Med 113:**220–228, 2002
22. Pappou IP, Papadopoulos EC, Swanson AN, Cammisa FP Jr, Girardi FP: Osteoporotic vertebral fractures and collapse with intravertebral vacuum sign (Kümmel's disease). **Orthopedics 31:**61–66, 2008
23. Peh WC, Gelbart MS, Gilula LA, Peck DD: Percutaneous vertebroplasty: treatment of painful vertebral compression fractures with intraosseous vacuum phenomena. **AJR Am J Roentgenol 180:**1411–1417, 2003
24. Resnick D, Niwayama G, Guerra J Jr, Vint V, Usselman J: Spinal vacuum phenomena: anatomical study and review. **Radiology 139:**341–348, 1981
25. Saita K, Hoshino Y, Kikkawa I, Nakamura H: Posterior spinal shortening for paraplegia after vertebral collapse caused by osteoporosis. **Spine 25:**2832–2835, 2000
26. Sarli M, Pérez Manghi FC, Gallo R, Zanchetta JR: The vacuum cleft sign: an uncommon radiological sign. **Osteoporos Int 16:**1210–1214, 2005
27. Suk SI, Kim JH, Lee SM, Chung ER, Lee JH: Anterior-posterior surgery versus posterior closing wedge osteotomy in posttraumatic kyphosis with neurologic compromised osteoporotic fracture. **Spine 28:**2170–2175, 2003
28. Yu CW, Hsu CY, Shih TT, Chen BB, Fu CJ: Vertebral osteonecrosis: MR imaging findings and related changes on adjacent levels. **AJNR Am J Neuroradiol 28:**42–47, 2007

Manuscript submitted April 28, 2009.
Accepted March 26, 2010.

Address correspondence to: Satoshi Kawaguchi, M.D., Department of Orthopaedic Surgery, Asahikawa Kosei Hospital, 111-3, 1-jo 24-chome, Asahikawa 078-8211, Japan. email: kawaguch@sapmed.ac.jp.

J Bone Miner Metab (2010) 28:561–567
DOI 10.1007/s00774-010-0164-5

ORIGINAL ARTICLE

Effects of raloxifene treatment on the structural geometry of the proximal femur in Japanese women with osteoporosis

Junichi Takada · Takami Miki · Yasuo Imanishi · Kiyoshi Nakatsuka · Hiroshi Wada · Hiroshi Naka · Takashi Yoshizaki · Kousuke Iba · Thomas J. Beck · Toshihiko Yamashita

Received: 20 November 2009 / Accepted: 24 January 2010 / Published online: 24 March 2010

Abstract The purpose of this study was to clarify the effects of 2-year treatment with raloxifene on the proximal femoral geometry among Japanese patients with osteoporosis by hip structure analysis. One hundred ninety-eight community-dwelling postmenopausal women with osteoporosis were enrolled. The structural variables were areal bone mineral density (BMD), cross-sectional area (CSA), section modulus (index of resistance to bending forces), and buckling ratio (index of cortical instability). BMD, CSA, and section modulus at the narrow neck significantly increased by 1.27, 2.67, and 3.90% at 2 years, respectively. BMD, CSA, and section modulus at the intertrochanter significantly increased by 2.55, 4.49, and 6.60% at study termination, respectively. The buckling ratio at the intertrochanter decreased by 2.36% at 1 year, but differences at 2 years became non-significant. Parameters at the shaft were qualitatively similar to those of the narrow neck and intertrochanter. The percent change of the section modulus was significantly higher than that of BMD at 2 years in all three regions. The percent changes of the section modulus is strongly correlated with the percent changes of BMD and CSA, and negative correlated with the percent changes of buckling ratio in all regions. In conclusion, Japanese osteoporotic women on raloxifene therapy have significant improvements of both BMD and geometry in the proximal femur.

Keywords Hip structure analysis · Raloxifene · Geometry · Bone strength · Hip fracture

J. Takada · K. Iba · T. Yamashita
Department of Orthopedic Surgery, Sapporo Medical University, Sapporo, Japan

J. Takada (✉) · T. Yoshizaki
Kitago Orthopedic Clinic, Sapporo, Japan
e-mail: jtakada@kitago-ortho.com

T. Miki · H. Naka
Department of Geriatrics, Osaka City University, Osaka, Japan

Y. Imanishi
Department of Metabolism, Endocrinology, and Molecular Medicine, Osaka City University Graduate School of Medicine, Osaka, Japan

K. Nakatsuka
Nozaki Clinic, Osaka, Japan

H. Wada
Wada Obstetrics and Gynecology Clinic, Asahikawa, Japan

T. J. Beck
Department of Radiology, The Johns Hopkins University, Baltimore, MD, USA

Introduction

Areal bone mineral density (BMD) measured by dual energy X-ray absorptiometry (DXA) is a valuable tool for the evaluation of bone fragility and shows significant correlations between BMD decline and risk of fracture [1–3]. However, BMD may not be the best assessment of treatment efficacy since the fracture reduction after treatment is only partially explained by increased BMD [4–6]. Strength of bone is however governed by structural dimensions and tissue materials properties, neither of which is directly measured by a conventional BMD measurement. Beck and Ruff have applied the hip structure analysis (HSA) method to measure proximal femur geometry and strength using conventional DXA scans of the hip [7, 8]. HSA has been

used to demonstrate age trends, racial and gender differences, and treatment effects on osteoporosis in Caucasians [8–16]. In Japan, we have previously demonstrated age-related differences in structural geometry and femoral strength and changing patterns in HSA geometry that may be consistent with the epidemiological evidence of hip fracture rates in Japan [17]. However, osteoporosis treatments analyzed by HSA have not previously been reported in Japanese patients.

The purpose of this study was to use the HSA method to gain some insights into the effects of a 2-year treatment with raloxifene on the proximal femur geometry among Japanese women with osteoporosis.

Materials and methods

One hundred ninety-eight community-dwelling, ambulatory, postmenopausal women were enrolled who had osteoporosis as defined by Japanese diagnostic criteria [18]. These criteria included low BMD (T score < -2.5) or presence of osteoporotic fractures. Patients with a history of hip fracture or any disease or medication known to affect bone metabolism were excluded from this study. All patients were given raloxifene (60 mg/day) over the study period.

DXA scans of the hip were taken at baseline, and were repeated at 6-, 12-, and 24-month follow-up points. Hip scans were performed using a hip positioner system (HPS; OsteoDyne, Durham, NC) to ensure consistent positioning [19]. This device keeps the subject's legs positioned in abduction and internal rotation (15°).

Hip structure analysis

The archived DXA images were analyzed using the HSA method, which has been described in detail in earlier publications [7, 8]. Briefly, DXA scan files were first converted into bone mass images in which pixel values represent bone mass in grams per square centimeter, using an automated program. The underlying principle of the method is that a line of pixels traversing the bone axis is a projection of the corresponding cross-section from which certain geometric properties can be derived.

Three measured sites were defined as (1) narrow neck, traversing the narrowest width of the femoral neck; (2) intertrochanter, along the bisector of the shaft and femoral neck axes; (3) shaft, at a distance of 1.5 times the minimum neck width, distal to the intersection of the neck and shaft axes.

The structural variables used in this paper were as follows [20, 21].

- Areal BMD (g/cm^2): mean values of BMD from the narrow neck region are on average about 14% higher than the conventional Hologic neck ROI values on the same subjects, although age trends were similar in previous reports [10].
- Outer diameter (cm): the distance between (blur corrected) outer margins of the cross-section.
- Cross-sectional area (CSA, cm^2): this is defined as the surface area of bone tissue in the cross-section after excluding soft tissue (marrow) spaces. CSA is an index of resistance to forces directed along the long axis of the bone.
- Section modulus (cm^3): this is an index of resistance to bending forces and is calculated as CSMI/d_{max} where CSMI is the cross-sectional moment of inertia and d_{max} is the maximum distance from either bone edge to the centroid of the profile.
- Average cortex (cm): this is an estimate of the mean cortical thickness assuming a circular (narrow neck or shaft) or elliptical (intertrochanter) annulus model of the cross-section for use in the estimated buckling ratio. The model assumes that 60, 70, and 100% of the measured bone mass is in the cortex for the narrow neck, intertrochanter and shaft, respectively.
- Buckling ratio: this describes stable configurations of thin-walled tubes subjected to compressive loads and is estimated as the ratio of d_{max} to the estimated mean cortical thickness.

In addition to these parameters, the HSA program measures neck-shaft angle and femoral-neck length. The latter is defined as the distance from the center of the femoral head to the intersection of the neck and shaft axes.

Statistical analysis

All parameters are presented as mean (standard deviations, SD) at baseline and percent differences from baseline (95% confidence interval, CI). Differences were regarded as statistically significant when the 95% CI did not include zero. P values from two-sample t tests were employed to compare HSA parameter means. The correlations between HSA parameters were analyzed by Pearson's R and considered statistically significant at $P < 0.05$.

Results

Clinical characteristics at baseline

The mean (SD) age, body mass index, neck shaft angle, and neck length were 62.6 (7.7) years, 22.0 (3.0) kg/m^2, 129.1

(4.6) degrees, and 4.7 (0.5) cm, respectively. The neck-shaft angles and femoral-neck lengths were not significantly different from Japanese values (neck-shaft angle: 129.9°, femoral-neck length: 4.7 cm) from our previous report [17].

Changes from baseline in HSA parameters over 2 years

Based on repeated measures analyses, the baseline values and the percent changes from baseline in each parameter are shown in Tables 1, 2, and 3.

Narrow neck

BMD significantly increased by 1.27% (95% CI: 0.01, 2.54) compared to baseline at 2 years. The section modulus, an index of bending strength, significantly increased by 2.53% (95% CI: 1.22, 3.85) and 3.90% (95% CI: 2.33, 5.47) compared to baseline at 1 and 2 years, respectively. Compared to baseline, the mean difference in CSA was 1.20% (95% CI: 0.32, 2.08) after 1 year and 2.67% (95% CI: 1.44, 3.90) at study termination. Outer diameter significantly increased at study termination; however, changes in average cortex and buckling ratio did not reach significance (Table 1).

Intertrochanter

BMD increased significantly by 2.73% (95% CI: 1.88, 3.58) at 1 year and then remained relatively constant thereafter by 2.55% (95% CI: 1.55, 3.55) at study termination. The section modulus significantly increased by 4.63% (95% CI: 3.38, 5.87) and 6.60% (95% CI: 4.93, 8.26) compared to baseline at 1 and 2 years, respectively. The buckling ratio decreased by 2.36% (95% CI: −3.55, −1.16) at 1 year, but differences at 2 years became non-significant (−0.69%, 95% CI; −2.05, 0.66). The other parameters, CSA, outer diameter, and average cortex, were all significantly increased at study termination by 4.49% (95% CI: 3.30, 5.67), 1.92% (95% CI: 1.07, 2.78), and 2.78% (95% CI: 1.44, 4.12), respectively (Table 2).

Shaft

Results at the femoral shaft were qualitatively similar to those of the narrow neck and intertrochanter. The effects of raloxifene were significantly increased in all parameters except buckling ratio at study termination (Table 3).

It is worth noting that the % change of the section modulus was significantly higher than that of BMD at 2 years in all three regions.

Table 1 Mean (SD) bone values at baseline and mean percent difference (95% CI) from baseline in raloxifene treatment in 2 years at the narrow neck region

Narrow neck	Baseline values, mean (SD)	% difference vs. baseline, mean (95% CI)		
		6 months	12 months	24 months
BMD (g/cm^2)	0.742 (0.134)	0.03 (−0.81, 0.87)	0.47 (−0.50, 1.45)	1.27 (0.01, 2.54)*
CSA (cm^2)	2.033 (0.351)	0.89 (−0.14, 1.92)	1.20 (0.32, 2.08)*	2.67 (1.44, 3.90)*
Outer diameter (cm)	2.889 (0.186)	0.85 (0.39, 1.30)*	0.81 (0.25, 1.36)*	1.44 (0.68, 2.20)*
Section modulus (cm^3)	0.875 (0.165)	1.68 (0.14, 3.22)*	2.53 (1.22, 3.85)*	3.90 (2.33, 5.47)*
Average cortex (cm)	0.142 (0.027)	0.00 (−0.89, 0.89)	0.51 (−0.53, 1.55)	1.28 (−0.06, 2.61)
Buckling ratio	11.601 (0.118)	1.72 (0.61, 2.84)*	1.38 (−0.41, 3.17)	0.56 (−1.73, 2.81)

* $P < 0.05$ vs. baseline

Table 2 Mean (SD) bone values at baseline and mean percent difference (95% CI) from baseline in raloxifene treatment in 2 years at the intertrochanter region

Intertrochanter	Baseline values, mean (SD)	% difference vs. baseline, mean (95% CI)		
		6 months	12 months	24 months
BMD (g/cm^2)	0.749 (0.134)	2.12 (1.53, 2.87)*	2.73 (1.88, 3.58)*	2.55 (1.55, 3.55)*
CSA (cm^2)	3.507 (0.593)	2.15 (1.36, 2.94)*	3.53 (2.64, 4.41)*	4.49 (3.30, 5.67)*
Outer diameter (cm)	4.937 (0.343)	−0.02 (−0.56, 0.52)	0.82 (0.24, 1.41)*	1.92 (1.07, 2.78)*
Section modulus (cm^3)	2.903 (0.552)	2.29 (1.22, 3.36)*	4.63 (3.38, 5.87)*	6.60 (4.93, 8.26)*
Average cortex (cm	0.305 (0.059)	2.50 (1.65, 3.36)*	3.24 (2.15, 4.33)*	2.78 (1.44, 4.12)*
Buckling ratio	9.510 (2.346)	−2.38 (−3.20, −1.56)*	−2.36 (−3.55, −1.16)*	−0.69 (−2.05, 0.66)

* $P < 0.05$ vs. baseline

Table 3 Mean (SD) bone values at baseline and mean percent difference (95% CI) from baseline in raloxifene treatment in 2 years at the shaft region

Shaft	Baseline values, mean (SD)	% difference vs. baseline, mean (95% CI)		
		6 months	12 months	24 months
BMD (g/cm^2)	1.258 (0.218)	1.33 (0.65, 2.00)*	1.77 (0.89, 2.66)*	1.80 (0.76, 2.84)*
CSA (cm^2)	3.284 (0.527)	1.18 (0.48, 1.87)*	2.27 (1.43, 3.10)*	3.54 (2.48, 4.59)*
Outer diameter (cm)	2.754 (0.182)	−0.14 (−0.43, 0.15)	0.54 (0.07, 1.00)*	1.74 (1.18, 2.31)*
Section modulus (cm^3)	1.693 (0.312)	0.47 (−0.51, 1.45)	2.56 (1.36, 3.77)*	4.74 (3.26, 6.23)*
Average cortex (cm)	0.465 (0.105)	1.81 (0.92, 2.71)*	2.44 (1.12, 3.75)*	2.08 (0.62, 3.55)*
Buckling ratio	3.234 (0.919)	−1.59 (−2.60, −0.58)*	−1.26 (−2.79, 0.28)	0.11 (−1.55, 1.78)

* $P < 0.05$ vs. baseline

Table 4 Cross-correlations (Pearson's R) among the percent changes of parameters in hip structure analysis at the narrow neck region

Narrow neck	BMD	CSA	Outer diameter	Section modulus	Average cortex	Buckling ratio
BMD	1.000	0.840**	−0.465**	0.794**	0.998**	−0.862**
CSA		1.000	0.084	0.797**	0.825**	−0.520**
Outer diameter			1.000	−0.172*	−0.486**	0.769**
Section modulus				1.000	0.785**	−0.648**
Average cortex					1.000	−0.869**
Buckling ratio						1.000

* $P < 0.05$, ** $P < 0.001$

Table 5 Cross-correlations (Pearson's R) among the percent changes of parameters in hip structure analysis at the intertrochanteric region

Intertrochanter	BMD	CSA	Outer diameter	Section modulus	Average cortex	Buckling ratio
BMD	1.000	0.761**	−0.297**	0.535**	0.714**	−0.837**
CSA		1.000	0.392**	0.879**	0.894**	−0.708**
Outer diameter			1.000	0.534**	0.302**	0.148
Section modulus				1.000	0.757**	−0.557**
Average cortex					1.000	−0.868**
Buckling ratio						1.000

** $P < 0.001$

Table 6 Cross-correlations (Pearson's R) among the percent changes of parameters in hip structure analysis at the shaft region

Shaft	BMD	CSA	Outer diameter	Section modulus	Average cortex	Buckling ratio
BMD	1.000	0.865**	−0.360**	0.628**	0.975**	−0.909**
CSA		1.000	0.155	0.856**	0.803**	−0.598**
Outer diameter			1.000	0.357**	−0.416**	0.682**
Section modulus				1.000	0.561**	−0.361**
Average cortex					1.000	−0.914**
Buckling ratio						1.000

** $P < 0.001$

Correlations among the percent changes of parameters

Tables 4, 5, and 6 show correlations (Pearson's R) among the percent changes of HSA parameters in the narrow neck, intertrochanter, and shaft, respectively. The percent change of the section modulus is strongly correlated with the percent change of BMD, CSA, and average cortex and negatively correlated with the percent change of the

buckling ratio in all regions. As expected, the percent change of BMD has a positive relationship with the percent change of CSA, but a negative relationship with the percent change of outer diameter in all regions.

Discussion

One of the problems with the use of BMD as a monitor for osteoporosis treatment is that it does not completely capture the mechanical factors that lead to fragility [4–6]. On the other hand, bone geometry measurements have a more direct relationship with mechanical strength. In this study, we are the first to report that Japanese women on raloxifene therapy over 2 years had significant positive changes in the structural geometry at all measured cross sections of the proximal femur. Raloxifene treatment produced positive changes in CSA and in the section modulus, indices of geometric strength in axial compression and bending, respectively. These changes were particularly evident at the narrow neck and intertrochanter regions that correspond to common fracture sites. The interpretation of these data is complex because the interplay between structure and fragility is not completely understood.

It is critical to first consider the effect of periosteal expansion because it is a geometric confounder of BMD, but also opposing effects on bending resistance (section modulus) susceptibility. The expansion of bone outer diameters confounds conventional BMD analyses because it increases the region area over which the BMD is averaged (i.e., BMD = bone mineral content/region area). Thus, in general, any net gain in bone within cross sections due to treatment will be underestimated by BMD. This was the case in the present study as treatment-induced gain in bone (directly measured as CSA in HSA) is roughly twice that apparent in the BMD due to the effects of expansion (Tables 1, 2, 3). An increase in CSA will improve its resistance to the axial component of those loads. Under most conditions, however, bending dominates physiologic loads on the proximal femur, and addition of bone to the outer surface has a preferentially greater effect on the section modulus. In the present study, the treatment-induced effect on bending resistance (section modulus) is about 30–50% greater than the effect on CSA and 2–3 times the effect on BMD in the same region.

Outer diameters widened from baseline in all three femur regions, becoming significant after 12 months. Lack of a placebo group in the present study prevents drawing conclusions regarding treatment effects on expansion. The yearly changes of outer diameter in the present study were higher than that of literally reported data in untreated Japanese women (narrow neck: 0.46%/year, intertrochanter: 0.22%/year, shaft: 0.16%/year) [17]. However, it could not be concluded that the expansion of outer diameter in this study was the effect of raloxifene, because the literally reported data include not only osteoporotic patients, but also normal women, and the baseline values in this study were lower than those in literal data. In addition, the multiple outcomes of raloxifene evaluation (MORE) trial was unable to detect raloxifene effects on rates of periosteal apposition vs. placebo [12]. For the above-mentioned reasons, the expansion of outer diameter in the present study might mainly appear to accompany the aging process rather than the effects of raloxifene.

Nevertheless, the presence of expansion in the present study does have important implications because it modifies the effects of bone gain due to treatment. Although the outer diameter expands with age in untreated patients, average cortex, CSA, and section modulus decrease with age. On the other hand, the average cortex, CSA, and section modulus in raloxifene treatment were significantly increased. These results indicated that raloxifene decreased the bone resorption in endocortical bone without inhibiting the bone formation in periosteal, and induced an increase in the average cortex, CSA and section modulus.

Our results in Japanese women were generally consistent with the larger MORE study of raloxifene effects on a mostly (95.7%) white population of postmenopausal women with osteoporosis [12] with one notable difference. In both studies, significant improvements (reduction) in buckling ratios were evident at the narrow neck and intertrochanter regions at early time points, but differences declined with time. In the MORE study, a 2% lower buckling ratio remained significant at 3 years [12], but in our study, the buckling ratios were no longer significant after 2 years of treatment. A clinical trial by Greenspan et al. [13] evaluated the effects of estrogen replacement therapy on femur geometry, and showed positive effects on CSA and section modulus that were comparable to those of the present study. Interestingly, after 3 years of estrogen treatment, there were no apparent differences from baseline in buckling ratio at the narrow neck, intertrochanter, and shaft regions. Treatments followed for longer periods seem to initially reduce the buckling ratio, but with continued expansion the effect seems to moderate with time [12, 16, 22]. This mechanism still needs to be carefully studied.

MORE and the present study showed significantly improved geometric parameters in the proximal femur, which were similar to those of alendronate, risedronate, and estrogen, so that the important question is whether these results lead to a reduction of the incidence of hip fracture. In previous clinical trials, alendronate, risedronate, and estrogen have shown protective effects against hip fracture, but there are no reports about raloxifene for the reduction of hip fractures [23–28]. Alendronate, risedronate, and raloxifene (MORE) significantly improved

both the section modulus and buckling ratio, and the results for estrogen and the present study have shown significantly increased section modulus. These data indicated that there is no qualitative difference in the changes of geometric parameters (section modulus, buckling ratio) between raloxifene and others (alendronate, risedronate, estrogen). On the other hand, alendronate significantly improved the section modulus and buckling ratio compared to risedronate in a head-to-head trial [15]. However, these quantitative differences could not directly explain the risk reduction of hip fracture, because there is no evidence that alendronate has a superior effect for reducing hip fracture compared to risedronate. The quantitative differences between raloxifene and others (alendronate, risedronate, and estrogen) could not explain the risk reduction of hip fracture, because there is no head-to-head comparison study.

The MORE trial has shown that raloxifene treatments reduce new vertebral fracture incidence by about half compared to placebo control [23, 24], but the incidence of hip fracture in that trial was inadequate to detect effects on hip fracture rates. This contrasts with the alendronate (FIT-1) and risedronate (HIP) studies, where because of differences in enrollment criteria, rates of hip fracture in control groups were 3–5 times higher in the FIT-1 (2.2%) and HIP (3.2%) studies vs. 0.7% in MORE [23, 25, 26]. Nakamura et al. [29] reported that raloxifene treatment at 60 mg/day for 1 year resulted in a significant reduction in the risk of new clinical vertebral fractures and any new clinical fracture in postmenopausal Asian women with osteoporosis. Moreover, in a recent observational study, there were no significant differences in hip fracture incidence between patients treated with risedronate, raloxifene, and alendronate [30]. Raloxifene may reduce the incidence of hip fracture as well as risedronate and alendronate, although this would be difficult to prove in a head-to-head study because of the low incidence of hip fracture and the necessity for enrolling huge numbers of patients.

There are methodological limitations to our study; DXA scanners are not designed or optimized to measure structural dimensions. Precision, not evaluated in the present study, was relatively poor in the MORE study [12]. The main reason is the difficulty in reproducing the position of the three-dimensional femur in two-dimensional images separated months to years apart. Imprecision may prevent the detection of subtle effects on geometry in this study. In addition, use of two-dimensional DXA scans means that the section modulus is assessed only in the scan plane; effects of treatment may be different for bending directions out of the image plane.

Although there were some limitations, this study also has significant strengths. This is the first study employing the HSA method to examine geometric strength-related parameters in elderly Japanese women on raloxifene therapy over 2 years. Although these women maintained their hip BMD, there were statistically significant changes in the underlying geometry that have not previously been reported in this population. It is clear that like other osteoporosis treatments, raloxifene alters femur geometry in a positive direction. If technological improvements can make them reliable enough for clinical use, geometric measurements may ultimately provide a clearer view of the pharmacological efficacy of osteoporosis treatments.

We conclude that Japanese women on raloxifene therapy have significant improvements of both BMD and proximal hip structural geometry. Women who were treated with raloxifene showed positive structural changes in the proximal regions of the femur that suggest improved bending and axial strength over 2 years.

Acknowledgments The authors wish to acknowledge Mr. Etsuro Hamaya of Eli Lilly & Co. Lilly Research Laboratories, Japan, for his assistance.

References

1. Kanis JA (2002) Diagnosis of osteoporosis and assessment of fracture risk. Lancet 359:1929–1936
2. Miller PD (2003) Bone mass measurements. Clin Geriatr Med 19:281–297
3. Schott AM, Cormier C, Hans D, Favier F, Hausherr E, Dargent-Molina P, Delmas PD, Ribot C, Sebert JL, Breart G, Meunier PJ, EPIDOS Group (1998) How hip and whole-body bone mineral density predict hip fracture in elderly women: the EPIDOS prospective study. Osteoporos Int 8:247–254
4. Li Z, Meredith MP, Hoseyni MS (2001) A method to assess the proportion of treatment effect explained by a surrogate endpoint. Stat Med 20:3175–3188
5. Cummings SR, Karpf DB, Harris F, Genant HK, Ensrud K, LaCroix AZ, Dennis M, Black DM (2002) Improvement in spine bone density and reduction in risk of vertebral fractures during treatment with antiresorptive drugs. Am J Med 112:281–289
6. Sarkar S, Mitlak BH, Wong M, Stock JL, Black DM, Harper KD (2002) Relationships between bone mineral density and incident vertebral fracture risk with raloxifene therapy. J Bone Miner Res 17:1–10
7. Beck TJ, Ruff CB, Warden KE, Scott WW Jr, Rao GU (1990) Predicting femoral neck strength from bone mineral data: a structural approach. Investig Radiol 25:6–18
8. Beck TJ, Ruff CB, Scott WW Jr, Plato CC, Tobin JD, Quan CA (1992) Sex differences in geometry of the femoral neck with aging: a structural analysis of bone mineral data. Calcif Tissue Int 50:24–29
9. Beck TJ, Ruff CB, Bissessur K (1993) Age-related changes in female femoral neck geometry: implications for bone strength. Calcif Tissue Int 53:S41–S46
10. Beck TJ, Looker AC, Ruff CB (2000) Structural trends in the aging femoral neck and proximal shaft: analysis of the third national health and nutrition examination survey dual-energy X-ray absorptiometry data. J Bone Miner Res 15:2297–2304
11. Wang XF, Duan Y, Beck TJ, Seeman E (2005) Varying contributions of growth and ageing to racial and sex differences in femoral neck structure and strength in old age. Bone 36:978–986

12. Uusi-Rasi K, Beck TJ, Semanick LM, Daphtary MM, Crans GG, Desaiah D, Harper KD (2006) Structural effects of raloxifene on the proximal femur: results from the multiple outcomes of raloxifene evaluation trial. Osteoporos Int 17:575–586
13. Greenspan SL, Beck TJ, Resnick NM, Bhattacharya R, Parker RA (2005) Effect of hormone replacement, alendronate, or combination therapy on hip structure geometry: a 3-year, double blind, placebo-controlled clinical trial. J Bone Miner Res 20:1525–1532
14. Uusi-Rasi K, Semanick LM, Zanchetta JR, Bogado CE, Eriksen EF, Sato M, Beck TJ (2005) Effects of teriparatide [rh PTH (1–34)] treatment on structural geometry of the proximal femur in elderly osteoporotic women. Bone 36:948–958
15. Bonnick SL, Beck TJ, Cosman F, Hochberg MC, Wang H, de Papp AE (2009) DXA-based hip structural analysis of once-weekly bisphosphonate-treated postmenopausal women with low bone mass. Osteoporos Int 20:911–921
16. Beck TJ, Lewiecki EM, Miller PD, Felsenberg D, Liu Y, Ding B, Libanati C (2008) Effects of denosumab on the geometry of the proximal femur in postmenopausal women in comparison with alendronate. J Clin Densitom 11:351–359
17. Takada J, Beck TJ, Iba K, Yamashita T (2007) Structural trends in the aging proximal femur in Japanese postmenopausal women. Bone 41:97–102
18. Osteoporosis diagnostic criteria review committee: Japanese society for bone, mineral research (2001) Diagnostic criteria for primary osteoporosis: year 2000 revision. J Bone Miner Metab 19:331–337
19. Hans D, Duboeuf F, Schott AM, Horn S, Avioli LV, Drezner MK, Meunier PJ (1997) Effects of a new positioner on the precision of hip bone mineral density measurements. J Bone Miner Res 12:1289–1294
20. Ruff CB, Hayes WC (1983) Cross-sectional geometry of Pecos Pueblo femora and tibiae—a biomechanical investigation. I. Method and general patterns of variation. Am J Phys Anthropol 60:359–381
21. Melton LJ III, Beck TJ, Amin S, Khosla S, Achenbach SJ, Oberg AL, Riggs BL (2005) Contributions of bone density and structure to fracture risk assessment in men and women. Osteoporos Int 16:460–467
22. Chen Z, Beck TJ, Cauley JA, Lewis CE, LaCroix A, Bassford T, Wu G, Sherrill D, Going S (2008) Hormone therapy improves femur geometry among ethnically diverse postmenopausal participants in the Women's Health Initiative hormone intervention trials. J Bone Miner Res 23:1935–1945
23. Ettinger B, Black DM, Mitlak BH, Knickerbocker RK, Nickelsen T, Genant HK, Christiansen C, Delmas PD, Zanchetta JR, Stakkestad J, Glüer CC, Krueger K, Cohen FJ, Eckert S, Ensrud KE, Avioli LV, Lips P, Cummings SR, Multiple Outcomes of Raloxifene Evaluation Investigators (1999) Reduction of vertebral fracture risk in postmenopausal women with osteoporosis treated with raloxifene: results from a 3-year randomized clinical trial. JAMA 282:637–645
24. Delmas PD, Genant HK, Crans GG, Stock JL, Wong M, Siris E, Adachi JD (2003) Severity of prevalent vertebral fractures and the risk of subsequent vertebral and nonvertebral fractures: results from the MORE trial. Bone 33:522–532
25. Black DM, Cummings SR, Karpf DB, Cauley JA, Thompson DE, Nevitt MC, Bauer DC, Genant HK, Haskell WL, Marcus R, Ott SM, Torner JC, Quandt SA, Reiss TF, Ensrud KE, Fracture Intervention Trial Research Group (1996) Randomised trial of effect of alendronate on risk of fracture in women with existing vertebral fractures. Lancet 348:1535–1541
26. McClung MR, Geusens P, Miller PD, Zippel H, Bensen WG, Roux C, Adami S, Fogelman I, Diamond T, Eastell R, Meunier PJ, Wasnich RD, Greenwald M, Kaufman JM, Chesnut CH, Reginster JY (2001) Effect of risedronate on the risk of hip fracture in elderly women. N Engl J Med 344:333–340
27. Writing Group for the Women's Health Initiative Investigators (2002) Risks and benefits of estrogen plus progestin in healthy postmenopausal women: principal results from the women's health initiative randomized controlled trial. JAMA 288:321–333
28. The Women's Health Initiative Steering Committee (2004) Effects of conjugated equine estrogen in postmenopausal women with hysterectomy: the women's health initiative randomized controlled trial. JAMA 291:1701–1712
29. Nakamura T, Liu JL, Morii H, Huang QR, Zhu HM, Qu Y, Hamaya E, Thiebaud D (2006) Effects of raloxifene on clinical fractures in Asian women with postmenopausal osteoporosis. J Bone Miner Metab 24:414–418
30. Cadarette SM, Katz JN, Brookhart MA, Stümer T, Stedman MR, Solomon DH (2008) Relative effectiveness of osteoporosis drugs for preventing nonvertebral fracture. Ann Intern Med 148:637–646

骨粗鬆症に伴う痛みの治療

Treatment for pain associated with osteoporosis

特集

射場 浩介 IBA Kousuke
山下 敏彦* YAMASHITA Toshihiko

すべての医師のための骨粗鬆症診療ガイド2010
Key words 骨粗鬆症 腰背部痛 椎体骨折 骨性疼痛 ビスフォスフォネート

本邦における骨粗鬆症の有病率は，女性で24%，男性で5%であり，推定患者数は800万人を超える．主な臨床症候は，脆弱性骨折とそれに伴う疼痛・機能障害であり，骨粗鬆症患者の治療において骨折予防と疼痛改善が最も重要である[1]．今回は，骨粗鬆症に伴う痛みの治療について，腰背部痛を中心に概説する．

骨粗鬆症に伴う腰背部痛

骨粗鬆症に伴う腰背部痛には，①椎体骨折に伴う疼痛と，②骨粗鬆症自体の疼痛がある．前者はさらに，①椎体骨折による疼痛と，②脊柱変形に伴う慢性疼痛に分けられる．

1. 椎体骨折に伴う疼痛

1)椎体骨折による疼痛

椎体骨折を起こすほどの有害な機械的ストレスは，椎体とその周囲組織に分布する侵害受容器を刺激して急性疼痛を引き起こす．また，骨折部や周囲の損傷組織ではマクロファージなどの炎症性細胞が内因性発痛物質を放し，侵害受容器を興奮(excitation)・感作(sensitization)状態として急性・慢性疼痛を引き起こす．椎体骨折による疼痛は，骨癒合に伴い経時的に改善をする．一方，長期経過においても骨癒合を認めず，骨折部の不安定性を呈する椎体偽関節では，頑固な慢性疼痛を認める(図1)．当科における偽関節部組織の免疫組織学的検討では，炎症細胞浸潤や血管新生を認めた．脊柱の不安定性や椎体周囲の炎症などの要因が複合してポリモーダル受容器に作用し，頑固な腰背部痛をきたすものと推測された．

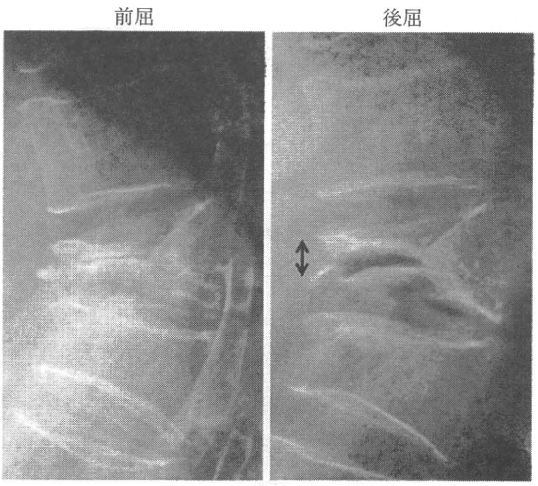

図1 第11胸椎椎体偽関節
椎体偽関節部は脊椎後屈で開大(矢印)を認める．

札幌医科大学医学部整形外科 講師 *教授

0371-1900/10/¥50/頁/JCOPY

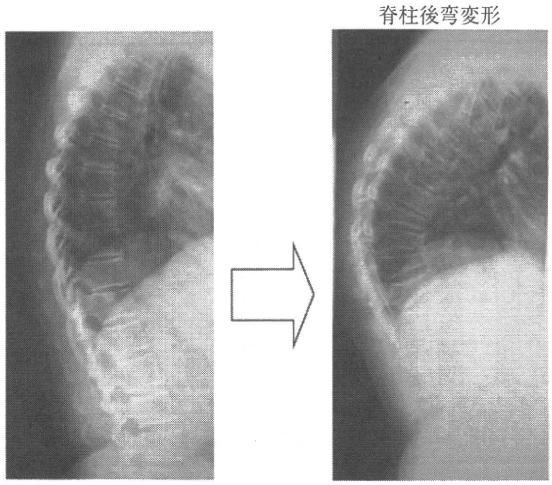

図2 多発性椎体骨折後に生じた脊柱後弯変形

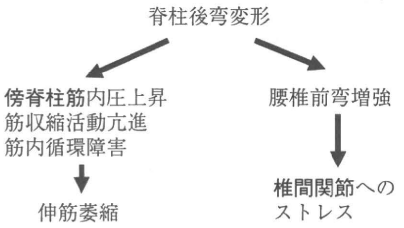

図3 脊柱後弯変形に伴う疼痛発生のメカニズム

2)脊柱変形に伴う疼痛

椎体骨折により胸腰椎の後弯変形が生じる(**図2**)と，傍脊柱筋の筋収縮活動が亢進するとともに，筋内圧が上昇する．さらに筋内循環障害，筋委縮が生じ，慢性腰痛の原因となる[2]．一方，胸椎後弯変形に対する腰椎の代償性前弯増強により，椎間関節に機械的ストレスがかかる(**図3**)．椎間関節には豊富に侵害受容器が存在しており，腰痛の発生源となる．

2. 骨粗鬆症自体による疼痛

最近の研究で，酸受容体であるカプサイシン受容体(TRPV1)陽性の神経線維[3]が骨髄内に分布することが明らかとなった(**図4**)．骨粗鬆症などの骨吸収亢進状態では，破骨細胞が活性化しており，骨吸収の際に形成される酸性環境がTRPV1を刺激して痛みを引き起こす[4]と考えられている(**図5**)．現在著者らは卵巣摘除(OVX)マウスを用

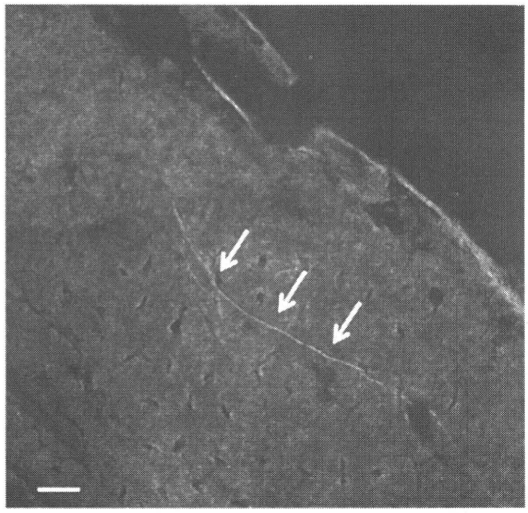

図4 抗TRPV1抗体による骨髄組織の免疫組織染色
TRPV1陽性の神経線維(白矢印)が骨髄内に分布することを確認した．(Niiyama, Kawamata, et al：unpublished data)

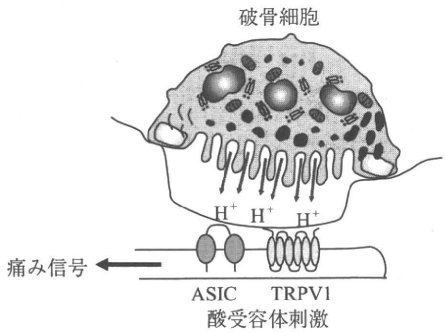

図5 破骨細胞が骨吸収時に形成する酸性環境が，骨髄内に分布する神経の酸受容体を刺激して痛み信号を発生する
(平賀 徹ほか：癌と骨病変(松本俊夫他編)，pp39-48，2004一部改変)

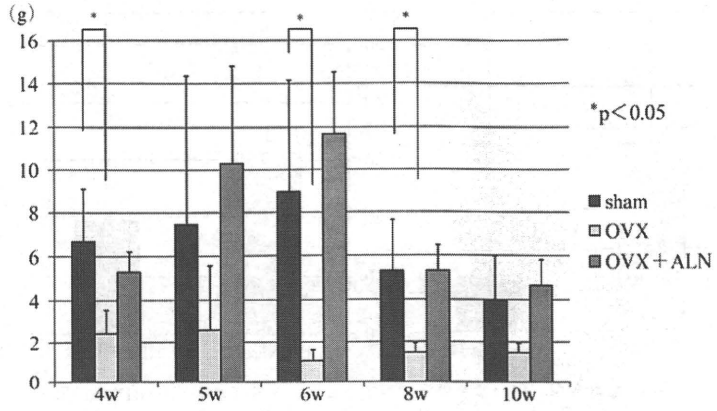

図6 OVX群はsham群と比較して疼痛域値の有意な低下を認め，さらにビスフォスフォネート投与で疼痛域値の改善を認めた
OVX後4，5，6，8，10週後にvon Frey testによる疼痛行動評価を行った．また，sham群，OVX後にビスフォスフォネートを投与した群(OVX＋ALN群)と疼痛域値を比較検討した．(Abe, et al：unpublished data)

いて，疼痛行動学的，免疫組織学的手法により，骨粗鬆症に伴う疼痛の発生メカニズムについて研究をすすめている．予備実験の段階ではあるが，疼痛行動学的検討においてOVXマウスは偽手術(sham)マウスと比較して疼痛閾値の低下を認めた．さらに，この低下した疼痛閾値は骨吸収抑制剤の投与で改善を認めた(図6)．このことは，骨粗鬆症に伴う疼痛の発生メカニズムを検討するうえで興味深い結果と考える．

骨粗鬆症に伴う痛みの治療

治療法には①薬物療法，②理学療法，③装具療法，④手術療法がある．疼痛を呈するそれぞれの病態に適した治療法の選択が必要となる．

1. 薬物療法

非ステロイド消炎鎮痛薬(NSAIDs)，ノイロトロピンや抗うつ薬(アミトリプチリンやタンドスピロン他)などの下行性疼痛抑制系賦活薬が用いられる．また，カルシトニンは破骨細胞の骨吸収を抑制する以外に，中枢性・末梢性の疼痛抑制効果を有することが知られている．

最近では，骨粗鬆症治療薬であるビスフォスフォネート(BP)や選択的エストロゲン受容体調節因子(SERM)が骨粗鬆症患者における腰背部痛を軽減することが報告されている[5]．これらの骨吸収抑制剤は，活性化した破骨細胞機能を抑制することで骨吸収亢進状態を改善する．そのため破骨細胞による酸性環境形成が障害され，酸受容体を介した疼痛刺激が減少する．以上のことが，BPやSERMが骨粗鬆症患者の疼痛を改善するメカニズムの1つとして考えられている．当科で行った検討でも，BP投与により骨粗鬆症患者の腰背部痛は有意に改善し，同時に骨吸収マーカーの低下を認めた(図7)．このことは骨吸収亢進状態を改善することが腰背部痛の改善に有用である可能性を示唆している．

2. 理学療法

物理療法として，温熱療法のホットパックや極超短波，電気療法としてTENSやSSP，レーザー治療などがあげられる．また，運動療法として，体幹筋力強化や全身的なストレッチングがすすめられる．

3. 装具治療

椎体骨折の急性期では疼痛改善と良好な骨癒合獲得のために，硬性・半硬性コルセット(図8)や体幹ギプスなどによる強固な外固定が重要であ

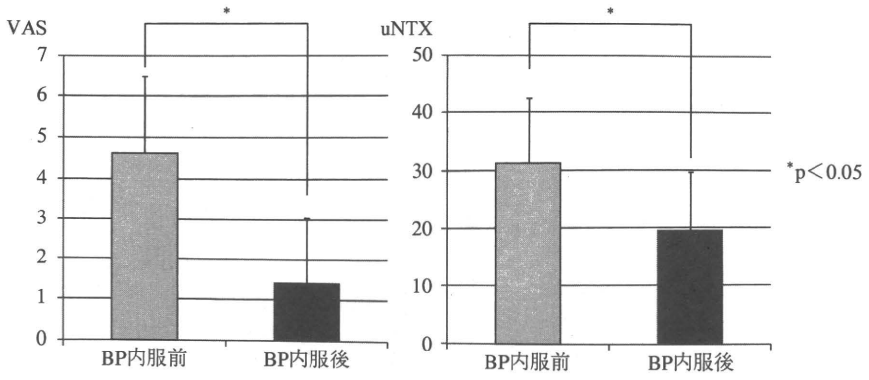

図7 骨粗鬆症に伴う腰背部痛に対するビスフォスフォネート(BP)の効果
腰背部痛は visual analogue scale(VAS)で評価を行い，骨代謝亢進状態の程度は尿中Ⅰ型コラーゲンN架橋テロペプチド(uNTX)で評価した．VASとuNTXはBP内服後に有意な低下を認めた．(当院骨粗鬆症外来での調査)

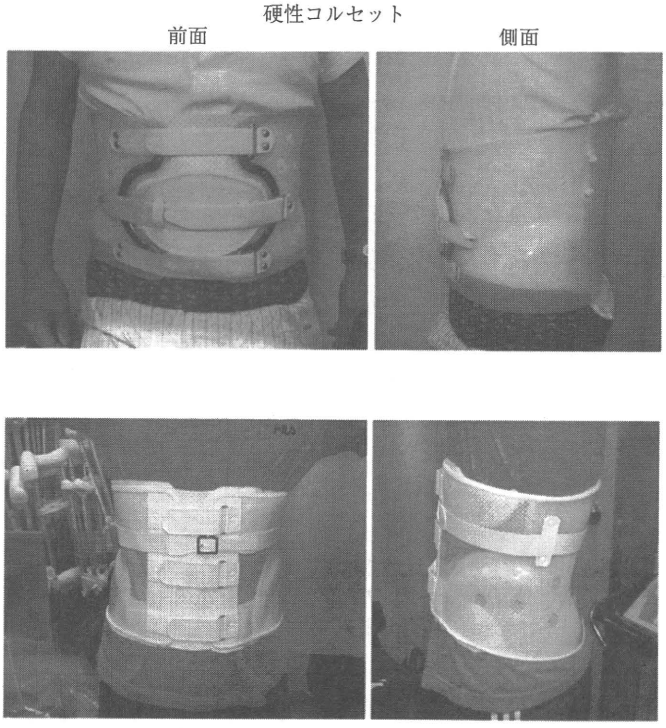

図8 硬性と半硬性コルセット

る．

4. 手術治療

骨粗鬆症性椎体骨折後に遅発性神経障害を認める症例や，椎体偽関節部の不安定性を呈する症例では手術が適応となる．手術法には脊椎前方固定手術，後方固定手術，椎体形成術がある．経皮的椎体形成術は低侵襲手術であること，術後早期に疼痛が改善することから骨粗鬆症性椎体骨折後の偽関節症例に対して広く行われている(**図9**)．

5. 慢性疼痛に対する治療

椎体骨折や脊柱変形を呈した症例のなかで，これまでに述べた治療で疼痛改善を認めない慢性疼